

Dynamical study of phase fluctuations and their critical slowing down in amorphous superconducting films

Wei Liu,¹ Minsoo Kim,² G. Sambandamurthy,² and N.P. Armitage¹

¹*Department of Physics and Astronomy, Johns Hopkins University, Baltimore, MD 21218*

²*Department of Physics, University at Buffalo-SUNY, 239 Fronczak Hall, Buffalo, NY 14260*

(Dated: June 30, 2021)

We report a comprehensive study of the complex AC conductance of amorphous superconducting InO_x thin films. We measure the explicit frequency dependency of the complex conductance and the phase stiffness over a range from 0.21 to 15 GHz at temperatures down to 350 mK using a novel broadband microwave Corbino spectrometer. The dynamic ac measurements are sensitive to the temporal correlations of the superconducting order parameter in the fluctuation range above T_c . Among other aspects, we explicitly demonstrate the critical slowing down of the characteristic fluctuation rate on the approach to the superconducting state and show that its behavior is consistent with vortex-like phase fluctuations and a phase-ordering scenario of the transition.

I. INTRODUCTION

The remarkable properties of superconductors and superfluids arise from the macroscopic quantum-mechanical coherence of their complex order parameter (OP), $\Psi = \Delta e^{i\phi}$. In conventional superconductors, fluctuations of the OP amplitude and phase occur in temperature regions only infinitesimally close to T_c . In contrast, in disordered materials with reduced dimensionality, the situation may be considerably different. Their low superfluid density gives a small phase stiffness and phase fluctuations that may be particularly soft.¹ In such systems, phase plays the role of a dynamic variable and may result in a situation where the transition results from a phase disordering of the order parameter while its amplitude remains finite. Effects such as zero resistivity are lost when the phase is no longer ordered on all lengths. However, phase correlations may remain over finite length and time scales resulting in significant precursor effects above T_c .

In strictly two dimensions (2D), such a transition has been proposed^{2,3} to be of the Kosterlitz-Thouless-Berezinskii (KTB) variety, as in ⁴He films.⁴⁻⁷ In such a transition, thermally excited free vortices are not possible below the transition temperature T_{KTB} as the vortex-antivortex binding energy increases logarithmically with separation. However, above T_{KTB} it becomes entropically favorable for vortices to unbind. Vortex pairs with the largest separation unbind first and the phase stiffness measured in the long-length and low-frequency limit suffers a discontinuous drop. Vortex unbinding reduces the global phase stiffness and renders the system increasingly susceptible to further vortex proliferation. At temperatures just above T_{KTB} such systems can be described as a two-component vortex plasma and may be realizations of the 2D XY model.

Because free vortices are the topological defects of the phase field, their spacing plays the role of a Ginzburg-Landau correlation length ξ , which diverges as $T \rightarrow T_{\text{KTB}}$. The role of free vortices as topological defects and their finite energy cost give an exponentially activated vortex density ($n_F \propto 1/\xi^2$). Asymptotically close to the

transition, this results in an unusually stretched exponential dependence of ξ on temperature, $\xi \sim e^{\sqrt{T/(T-T_{\text{KTB}})}}$, which is in stark contrast to the power laws typically expected near continuous phase transitions.⁵ Similar dependence is expected in the “critical slowing down” of the phase correlation time $1/\Omega$, which in a vortex plasma, is proportional to the time ξ^2/D required to diffuse the intervortex spacing (where D is the vortex diffusion constant).³

Although the conventional wisdom is that a KTB-like transition occurs in ultrathin superconducting films,² the issue is still in fact controversial. For instance, it has been proposed that, unlike ⁴He films, superconducting films are in a regime of low core energy (the high “fugacity” limit), that causes the transition to acquire a nonuniversal character or even be first order.⁷⁻⁹ There has been a great deal of work looking for KTB physics in the linear and nonlinear dc transport characteristics of thin films superconductors.¹⁰⁻¹² But it is not clear to what extent these experiments are influenced by inhomogeneous broadening¹³ and if even KTB physics would be detectable in such experiments.⁷ In contrast, finite-frequency measurements can directly probe temporal correlations and can be explicitly sensitive to phase fluctuations right above T_c . Important information has been gained from measurements at discrete frequencies,^{10,14-16} but only true spectroscopic measurements can give important information concerning critical slowing down.

In this paper, we present a comprehensive study of the complex ac conductance of effectively 2D amorphous superconducting InO_x films. We make use of our recent development of a broadband Corbino microwave spectrometer, which can measure the explicit frequency dependence of the complex conductance of thin films over a range from 0.21 – 15 GHz at temperatures down to 350 mK. These unique measurements allow true spectroscopy in the microwave range at low temperatures. We explicitly measure the temporal correlations of the fluctuation superconductivity and demonstrate the manner in which their time scales diverge on the approach to the transition. The temperature dependence of the critical slowing

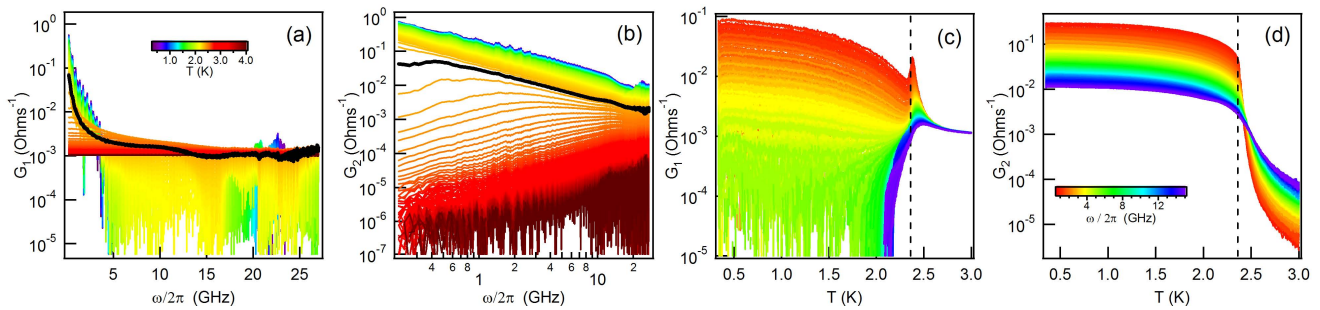


FIG. 1: (Color online) (a) and (b): frequency dependence of the real and imaginary conductances in the ranges $\omega/2\pi = 0.21 - 27$ GHz and $T = 0.35 - 4$ K. A color scale representing different temperatures is displayed in (a). The black curves are the conductances at T_c . The features in (a) at about 22 GHz are residual features imperfectly removed during calibration. (c) and (d): temperature dependence of the real and imaginary conductances in the frequency range $\omega/2\pi = 0.660 - 15$ GHz. A color scale representing different frequencies is displayed in (d). The dashed black lines mark $T_c = 2.36$ K.

down is consistent with a continuous transition induced by the freezing out of vortex-like phase fluctuations.

II. EXPERIMENTAL DETAILS

Experiments were performed in a broadband Corbino microwave spectrometer. This technique has been used previously to study high- T_c superconductor films, electron glasses, and heavy fermions.¹⁷⁻²¹ In this technique, a microwave signal is reflected by a sample that terminates the otherwise open-ended coaxial transmission line and is detected by a network analyzer. The measured complex reflection coefficient, S_{11}^m , has the contribution from both the transmission line and sample. The effects of extraneous reflections, damping, and phase shifts in the transmission line were compensated for by performing three reference measurements on standard samples as described elsewhere.^{22,23} A blank high-resistivity Si substrate was used as an open standard ($S_{11} = 1$). A 20-nm NiCr film evaporated on Si substrate was used as a load standard (its actual S_{11} can be evaluated from a simultaneous dc measurement). A 20-nm Nb film evaporated on Si substrate was used as a short standard ($S_{11} = -1$ when the Nb film is superconducting). The sample impedance, Z_S , can be calculated from the calibrated S_{11}^a via the standard expression $Z_S = \frac{1+S_{11}^a}{1-S_{11}^a} Z_0$, where $Z_0 = 50$ ohm is the characteristic cable impedance. The substrate contribution is taken into account as described in Ref. 24. For a thin film, where the sample thickness is much smaller than the skin depth, the complex conductivity is related to sample impedance as $\sigma = \frac{\ln(r_2/r_1)}{2\pi d Z_S}$, where r_2 and r_1 are the outer and inner radii of a donut-shaped sample and d is the thickness. A bias tee allows us to measure the two-contact dc resistance simultaneously with a lock-in amplifier. This measurement scheme was successfully incorporated into a ^3He cryostat. A particular experimental challenge was the heat sinking of the coaxial cable inner conductor. This was accomplished

through the inclusion of two hermetically sealed glass-bead adapters in the transmission line at the 4.2 K and ^3He stages separated by a short 10-cm-long superconducting NbTi coaxial cable. This system can probe the broadband microwave conductivity over the 0.05- to 15-GHz range at temperatures as low as 300 mK.

For these measurements, high-purity (99.999 %) In_2O_3 was e-gun evaporated under high vacuum onto clean high-resistivity silicon substrates to a thickness of approximately 30 nm. Our synthesis methods derive from the work of Ref.²⁵, where it was shown that amorphous InO_x can be reproducibly made by a combination of e-beam evaporation of In_2O_3 with optional annealing. Essentially similar films have been used in a large number of recent studies of the 2D superconductor-insulator quantum phase transition.^{14,26-30} We believe that the films are morphologically homogeneous with no crystalline inclusions or large-scale morphological disorder because of the following: TEM-diffraction patterns are diffuse rings with no diffraction spots, AFM images are completely featureless down to a scale of a few nanometers (the resolution of the AFM), and R versus T curves when investigating the 2D superconductor-insulator transition^{14,26} are smooth with no reentrant behavior that is the hallmark of gross inhomogeneity. The in-plane penetration depth — the so called Pearl length $(2\lambda_{3D}^2/d)^{31}$ — can be calculated from the data below to be approximately 6 mm near T_c , which is well in excess of any sample dimension. Vortices are therefore expected to have logarithmic interactions similar to the case of ^4He films.

III. RESULTS

In this paper, we concentrate on a particular InO_x film with a $T_c = 2.36$ K, but the data is broadly representative of samples with this normal-state resistance. In what follows, T_c is defined as the temperature at which the simultaneously measured dc resistivity becomes indistinguishable from zero (shown in Fig. 2). A small \pm

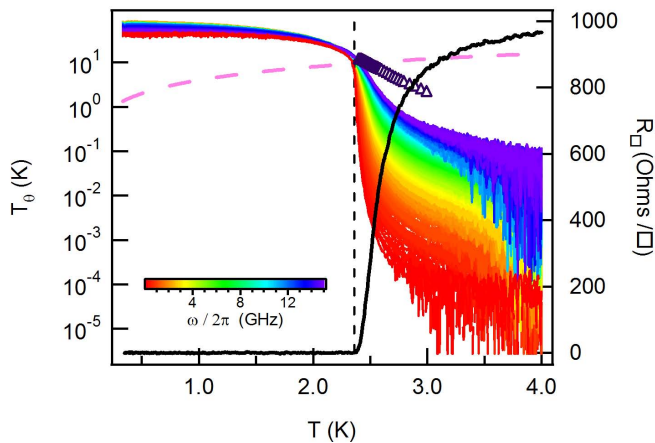


FIG. 2: (Color online) Temperature dependence of phase stiffness at $\omega/2\pi = 0.21 - 15$ GHz plotted against the vertical axis on the left. A color scale representing different frequencies is displayed as well. The black curve shows resistance per square of the same sample plotted with the vertical axis on the right. The dashed pink line is the KTB prediction, $4T_{\text{KTB}} = T_\theta$, for the universal jump in stiffness. The dark purple Δ markers are T_θ^0 s obtained via the scaling analysis described in the text. T_c is marked by the black dashed line.

5 mK uncertainty in this determination does not affect our conclusions. In Figs. 1 (a) and 1 (b) we plot the real (G_1) and imaginary (G_2) conductance as a function of frequency at different temperatures. Well above the transition, G_1 is flat and featureless and G_2 is small, as one expects for a highly disordered metal at low frequencies. When the sample is cooled toward T_c , the real conductance initially becomes enhanced and its spectral weight shifts to lower frequencies. At lower temperatures, the imaginary conductance grows dramatically and its frequency dependence becomes close to $1/\omega$. This is the low-temperature behavior expected for a superconductor.

As seen clearly in plots of the same data as a function of temperature [Fig. 1 (c) and (d)], the region immediately above T_c is dominated by superconducting fluctuations. As shown by comparison to the dashed line, the real and imaginary conductances begin to show an enhancement in the temperature region above T_c . Our measurements are explicitly sensitive to temporal correlations. This is seen for instance in the fact that the near- T_c “dissipation peak” in Fig. 1 (c) is exhibited at lower frequencies for lower temperatures; the maximum in dissipation is expected when the characteristic fluctuation rate $\Omega/2\pi$ is of the order of the probing frequency $\omega/2\pi$. The movement of the peak in temperature is a signature of critical slowing down in the raw data.

A particularly important quantity for quantifying fluctuations is the phase stiffness, which is the energy scale to twist the phase of the OP. The phase stiffness, T_θ , is proportional to the superfluid density and can be defined (in units of degrees Kelvin) through the imaginary

conductance G_2 as

$$k_B T_\theta(\omega) = \frac{G_2}{G_Q} \hbar \omega = \frac{N(\omega) e^2 \hbar d}{m G_Q}, \quad (1)$$

where $G_Q = \frac{4e^2}{h}$ is the quantum of conductance for Cooper pairs and $N(\omega)$ is a frequency-dependent effective density. In Fig. 2, we plot the stiffness versus temperature measured at frequencies between 0.21 to 15 GHz. $T_\theta(\omega)$ defined through Eq. (1) measures the stiffness on a length scale set by the probing frequency, which is typically proportional to the vortex diffusion length during a single radiation cycle, $\sqrt{\frac{\lambda D}{\omega/2\pi}}$. At temperatures well below T_c , there is essentially no frequency dependence to the phase stiffness, consistent with the scenario that the phase stiffness is rigid on all lengths. At temperatures slightly above T_c , the phase stiffness is largest at high frequencies. In the fluctuation regime, the system retains a phase stiffness on short length scales. Plotted alongside the stiffness data is the co-measured resistance per square, R_\square . Within experimental uncertainty, the phase acquires a frequency dependence at the temperature where the resistance appears to go to zero. In keeping with our discussion in the introduction, this is reasonable as a superconductor can only exhibit zero resistance when its phase is ordered on all lengths.

KTB theory predicts that at the transition temperature, T_{KTB} , the stiffness in the zero-frequency limit will have a discontinuous jump to zero with a magnitude $T_\theta = 4T_{\text{KTB}}$. However, because finite frequencies set a length scale, the ac stiffness should go to zero continuously. We generally expect that a signature of the discontinuity will manifest in a strong frequency dependence in the stiffness that onsets at T_{KTB} . In Fig. 2, the dashed diagonal line gives the prediction^{3,5} for the universal relationship between T_{KTB} and the stiffness. It crosses the stiffness curves very close to where they start to spread. This, along with the fact that the resistivity goes to zero at this temperature, leads us to assign the transition to a vortex unbinding transition of KTB-like character. Note that a careful inspection of Fig. 2 on linear scale reveals that the stiffness is in fact approximately 30% greater at T_c than the universal prediction. We cannot be sure at this time whether this is a systematic deviation (due perhaps to the dissipative motion of bound vortex pairs or evidence of a nonuniversal jump⁷) or a small calibration error.

Above T_{KTB} , the conductance due to fluctuating superconductivity is predicted^{3,19,32,33} to scale with the form

$$\frac{G(\omega)}{G_Q} = \left(\frac{k_B T_\theta^0}{\hbar \Omega} \right) S(\omega/\Omega). \quad (2)$$

In this scaling function, all temperature dependencies enter through Ω , the characteristic relaxation fluctuation rate, and T_θ^0 , an overall amplitude factor related to the

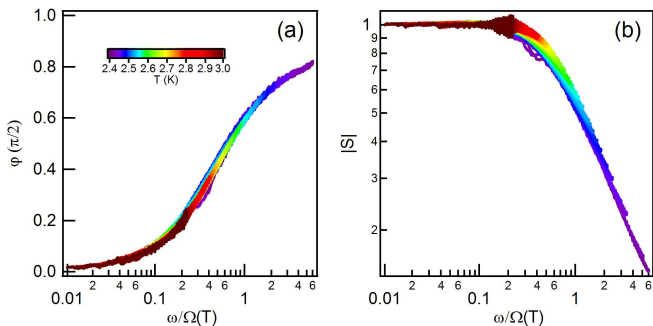


FIG. 3: (Color online) (a) Phase of $S(\omega/\Omega)$ normalized by $\pi/2$ as a function of reduced frequency ω/Ω . (b) Magnitude of $S(\omega/\Omega)$ as a function of reduced frequency. A color scale representing different temperatures for both plots is displayed in (a). Each plot is comprised of data measured at temperatures from 2.398 to 3 K and frequencies from 0.46 to 11 GHz.

total spectral weight in the fluctuating part of the conductivity. Note that in Eq. (2) the prefactors T_θ^0 and Ω are real quantities, so that the conductance phase angle, φ , must be equal to the phase angle of $S(\omega/\Omega)$. By scaling ω differently for each temperature, we can collapse the phase in a temperature range from 2.398 to 2.993 K into a single universal curve.

In Fig. 3 (a), we show this phase angle, φ , collapsed into a function of reduced frequency ω/Ω for each temperature. The data collapse reasonably well down to 38 mK above T_c . Below 38 mK, the fluctuation frequency begins to enter the low-frequency end of the spectrometer. In the low scaled-frequency limit, which corresponds to high temperatures and normal-state response, the phase approaches zero as expected. In the high scaled-frequency limit, which corresponds to low temperatures and the superconducting state, the phase approaches $\pi/2$ also as expected. This analysis allows us to extract $\Omega(T)$. Here, we have isolated the fluctuation contribution to the conductance by subtracting off the dc value from well above T_c (at 5.6 K). Having determined $\Omega(T)$, we adjust T_θ^0 and normalize the magnitude of conductance by $\frac{k_B T_\theta^0}{\hbar \Omega}$ to get the magnitude ($|S|$) of $S(\omega/\Omega)$ so that they fall onto one curve as demonstrated in Fig. 3 (b). In 2D, T_θ^0 is equivalent to the high-frequency limit of the stiffness. We plot it alongside the finite-frequency stiffness in Fig. 2.

The monotonic decrease of $\Omega(T)$ [Fig. 4 (a)] as T_c is approached from above, is an indication for the critical slowing down expected near a continuous transition. In Figs. 4 (b) and 4 (c), we fit $\Omega(T)$ to the stretched exponential form expected near a KTB transition $\Omega_0 \exp(-\sqrt{4T'/(T-T_c)})$ as well as to a generic power-law form $\Omega_0(1 - \frac{T}{T_c})^{z\nu}$. The fits were performed over different temperature ranges from T_c on up (147 and 112 mK, respectively) such that the same reduced χ^2 is achieved on both fits.

The stretched-exponential fit gives coefficients of $\Omega_0/2\pi = 181$ GHz and $T' = 0.23$ K, while the power-law

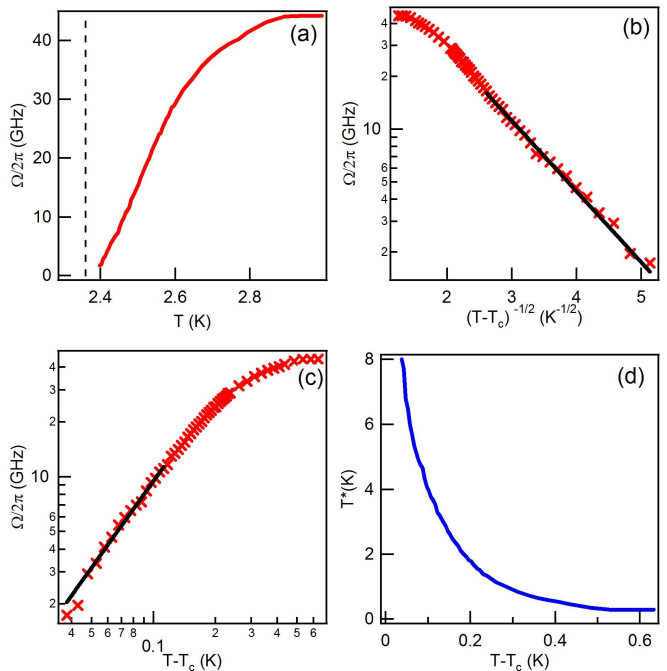


FIG. 4: (Color online) (a) Fluctuation frequency as a function of temperature from 2.398 to 2.993 K. In (b) and (c), we plot $\Omega(T)/2\pi$ versus $1/\sqrt{T-T_c}$ and $T-T_c$, respectively, along with the fitting (black curves). (d) Excitation energy in units of degrees Kelvin as a function of $T-T_c$.

fit gives $\Omega_0/2\pi = 90$ GHz and $z\nu = 1.58$, which are all reasonable parameters. For instance, within the ansatz of Ref. 3 it is predicted that $T' = \gamma(T_{c0} - T_{KTB})$, where γ is a constant of the order of unity. Ref. 13 predicts more specifically that $\gamma = 4\alpha^2$, where α is the ratio of the vortex core energy, μ , to the vortex core energy in the 2D XY model, μ_{xy} . Viewed in this regard, our value of T' is consistent with a reasonably small value of the core energy.

For both functional forms, one expects that the prefactor Ω_0 will be of order of the inverse time needed to diffuse a vortex with core size ξ_0 . Using the Bardeen-Stephen³ approximation for D , one can derive the expression $\hbar\Omega_0 = 2\pi\lambda\hbar D/\xi_0^2 = 2\pi\lambda\frac{G_Q}{G_N}k_B T_c$, where λ is a constant of the order of unity and G_N is the normal-state dc conductance. For the present sample, this gives $\Omega_0/2\pi \approx \lambda*48$ GHz, which is consistent with both fits. Due to its larger fitting range and its consistency with the universal jump, we favor the stretched exponential form, but in practice, it is difficult to definitively exclude power-law dependencies.

However, we can note a number of additional aspects consistent with a vortex plasma regime. Over a more extended temperature range above T_c , one expects that $\Omega(T)$ will obey the relation $\Omega_0 \exp(-\frac{T^*}{T})$. Here, T^* is half the energy needed to thermally excite a free vortex-antivortex pair. In Fig. 4 (d), we plot $T^* = T \ln(\Omega_0/\Omega)$. As expected this quantity appears to diverge as $T \rightarrow T_c$.

It reaches a high-temperature limiting value of about 0.27 K. One expects¹¹ that $k_B T^* = \mu + \frac{1}{2} k_B T_\theta^0 \ln(\xi/\xi_0)$ as the logarithmic interaction has a cutoff at ξ . At temperatures well above T_c where ξ is of the order of ξ_0 , the logarithmic term is negligible and the excitation energy should be proportional to the core energy alone. Within the BCS model, the core energy can be shown¹¹ to be approximately $k_B T_\theta^0(T)/8$. A comparison with T_θ^0 from Fig. 2 gives an estimate of $\mu/k_B \approx 0.3$ K in this temperature range. The agreement with experiment is essentially exact, but one should not take the exactness too seriously as there are a number of neglected factors of the order of unity.

IV. CONCLUSION

We have presented a comprehensive study of the complex microwave conductance of amorphous superconduct-

ing InO_x thin films. Our data explicitly demonstrate critical slowing down close to the phase transition and, in general, the applicability of a vortex-plasma model above T_c . This technique opens up the possibility of studying dynamic scaling of phase transitions at low temperatures and frequencies of a number of material systems.

V. ACKNOWLEDGEMENTS

We thank L. Benfatto, L.S. Bilbro, L. Engel, H. Kitano, M. Scheffler, R. Valdes Aguilar, and L. Zhu for helpful discussions. The research at JHU was supported by NSF DMR-0847652. The research at UB was supported by NSF DMR-0847324.

-
- ¹ V. Emery and S. Kivelson, *Nature (London)* **374**, 434 (1995).
- ² M. R. Beasley, J. E. Mooij, and T. P. Orlando, *Phys. Rev. Lett.* **42**, 1165 (1979).
- ³ B. Halperin and D. Nelson, *J. Low Temp. Phys.* **36**, 599 (1979).
- ⁴ V. Berezinskii, *Sov. Phys. JETP* **34**, 610 (1972).
- ⁵ J. Kosterlitz and D. Thouless, *J. Phys. C* **6**, 1181 (1973).
- ⁶ D. J. Bishop and J. D. Reppy, *Phys. Rev. Lett.* **40**, 1727 (1978).
- ⁷ P. Minnhagen, *Rev. Mod. Phys.* **59**, 1001 (1987).
- ⁸ J.-R. Lee and S. Teitel, *Phys. Rev. Lett.* **64**, 1483 (1990).
- ⁹ D. Y. Iz, V. N. Ryzhov, and E. E. Tareyeva, *Phys. Rev. B* **54**, 3051 (1996).
- ¹⁰ A. T. Fiory, A. F. Hebard, and W. I. Glaberson, *Phys. Rev. B* **28**, 5075 (1983).
- ¹¹ K. Epstein, A. M. Goldman, and A. M. Kadin, *Phys. Rev. B* **26**, 3950 (1982).
- ¹² J. W. P. Hsu and A. Kapitulnik, *Phys. Rev. B* **45**, 4819 (1992).
- ¹³ L. Benfatto, C. Castellani, and T. Giamarchi, *Phys. Rev. B* **80**, 214506 (2009).
- ¹⁴ R. W. Crane, N. P. Armitage, A. Johansson, G. Sambandamurthy, D. Shahar, and G. Grüner, *Phys. Rev. B* **75**, 094506 (2007).
- ¹⁵ R. Crane, N. P. Armitage, A. Johansson, G. Sambandamurthy, D. Shahar, and G. Grüner, *Phys. Rev. B* **75**, 184530 (2007).
- ¹⁶ H. Kitano, T. Ohashi, A. Maeda, and I. Tsukada, *Physica C: Superconductivity* **460**, 904 (2007), ISSN 0921-4534.
- ¹⁷ J. C. Booth, D. H. Wu, S. B. Qadri, E. F. Skelton, M. S. Osofsky, A. Piqué, and S. M. Anlage, *Phys. Rev. Lett.* **77**, 4438 (1996).
- ¹⁸ D. H. Wu, J. C. Booth, and S. M. Anlage, *Phys. Rev. Lett.* **75**, 525 (1995).
- ¹⁹ T. Ohashi, H. Kitano, I. Tsukada, and A. Maeda, *Phys. Rev. B* **79**, 184507 (2009).
- ²⁰ M. Lee and M. L. Stutzmann, *Phys. Rev. Lett.* **87**, 056402 (2001).
- ²¹ M. Scheffler, M. Dressel, J. Martin, and H. Adrian, *Nature (London)* **438**, 1135 (2005).
- ²² M. Scheffler, Ph.D. thesis, University of Stuttgart, (2004).
- ²³ H. Kitano, T. Ohashi, and A. Maeda, *Review of Scientific Instruments* **79**, 074701 (2008).
- ²⁴ J. Booth, Ph.D. thesis, University of Maryland at College Park, (1996).
- ²⁵ D. Kowal and Z. Ovadyahu, *Solid State Communications* **90**, 783 (1994).
- ²⁶ G. Sambandamurthy, L. W. Engel, A. Johansson, and D. Shahar, *Phys. Rev. Lett.* **92**, 107005 (2004).
- ²⁷ G. Sambandamurthy, L. W. Engel, A. Johansson, E. Peled, and D. Shahar, *Phys. Rev. Lett.* **94**, 017003 (2005).
- ²⁸ G. Sambandamurthy, A. Johansson, E. Peled, D. Shahar, P. Björnsson, and K. Moler, *EPL* **75**, 611 (2006).
- ²⁹ M. Steiner and A. Kapitulnik, *Physica C* **422**, 16 (2005).
- ³⁰ V. Gantmakher and M. Golubkov, *JETP Lett.* **73**, 131 (2001).
- ³¹ J. Pearl, *Applied Phys. Lett.* **5**, 65 (1964).
- ³² D. S. Fisher, M. P. A. Fisher, and D. A. Huse, *Phys. Rev. B* **43**, 130 (1991).
- ³³ J. Corson, R. Mallozzi, J. Orenstein, J. Eckstein, and I. Bozovic, *Nature (London)* **398**, 221 (1999).